

Piezoelectrically Activated Silicon Resonators

J. Baborowski, C.Bourgeois, A.Pezous, C.Muller, M.-A.Dubois

Microelectronic Division

CSEM SA

Neuchatel, Switzerland

jacek.baborowski@csem.ch

Abstract— This paper describes the feasibility and performances of two families of AlN/Si resonators: 1 MHz extensional and 20 to 100 kHz flexural resonators. In both components the resonating structure is obtained with SOI silicon suspended beams driven by an AlN piezoelectric layer. The 1MHz resonator exhibits a Q factor larger than 100 000 under vacuum and a coupling coefficient of 0.06%. The 20 to 100kHz resonators exhibit extremely low thermal drift of resonant frequency (α close to zero). The thermal compensation has been obtained at device-level by using SiO₂ with an appropriate thickness.

I. INTRODUCTION

Current wireless applications are setting increasing demands for the oscillators size, power consumption, and price. The conventional quartz crystal-based low-phase-noise oscillators are typically centimeter sized and appear bulky in the otherwise highly integrated transceiver architectures. Micromechanical resonators that exhibit very small change in resonant frequency over a broad temperature range and good stability over time offer a promise of compact size, low power consumption, and integrability with IC electronics, and are thus a very attractive potential alternative for the quartz crystals [1]. High Q silicon MEMS resonators have great potential for on-chip high frequency applications, integrated circuit clock generation, and other applications based on a stable frequency reference signal. The thermal compensation of the silicon resonator as well as the development of miniature inexpensive lead-free packaging solutions represent however real technical and scientific challenges.

The drawback of silicon resonators is their strong thermal drift. This effect is related to the negative thermal coefficient of stiffness (TCE), which is -65 to -60 ppm/°C, depending on the orientation [2]. Current developments for thermal compensation use very often an integrated thermometer, and require an individual calibration of each resonator [3]. Other methods are based on the control of the stiffness of the resonant structure to reduce the temperature coefficient of frequency (TCf) [4]. Composite structures with materials exhibiting positive and negative TCE can also be tailored for

thermal compensation at the device level [5]. The positive temperature coefficient of stiffness of silicon oxide is used for the compensation of the negative TCE of Si and of the other materials used in the vibrating structure.

The amount of SiO₂ necessary to obtain a close to zero TCf for the resonator depends on the shape of the resonator and the vibration mode. In some cases, up to 30% of the volume of the resonator has to be SiO₂, which can prove to be impractical for fabrication. Furthermore, it is usually detrimental to the Q factor, since defect-free single crystal is replaced by amorphous lossy material. The design of the resonator and the selection of the vibration mode must be done carefully as a function of the application specifications, knowing that the Q factor has to be traded against the reduction of TCf.

The excitation of silicon resonators is most often realized by electrostatic actuation [2,3,5,6]. The drawbacks include the relatively high supply voltage, and the non-linearity linked to the varying distance between the electrodes. An alternative actuation scheme uses the combination of a high quality piezoelectric thin film with a Si single crystal mechanical resonator. The use of aluminium nitride (AlN) as piezoelectric material enables to drive the resonator in a linear regime, and at low voltage, at the cost of a slightly more complicated fabrication flow.

This paper describes the feasibility and performances of a class of low frequency Si resonators operating between 20 kHz and 1 MHz, and driven by an AlN polycrystalline film. Both extensional resonators with very high Q factors, and thermally compensated flexural resonators are discussed.

II. PRINCIPLE

A. Longitudinal mode resonators

The first device presented in this paper is an in-plane extensional mode resonator. This resonator consists of a T-shaped silicon beam anchored at its base end, with an inertial mass at each extremity (Fig.1a). The driving voltage is applied

on the piezoelectric layer only in the horizontal part of the beam. Typically for a $1000 \times 250 \text{ } \mu\text{m}^2$ beam, the resonance frequency of the extensional mode is around 1 MHz.

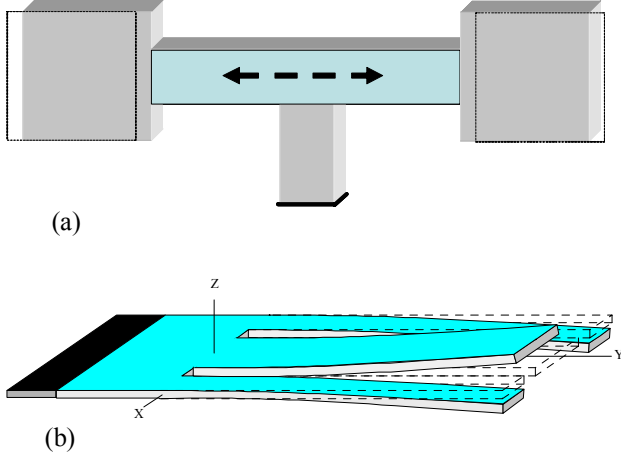


Figure 1. Schematic view of (a) extensional, (b) flexural mode resonators.

B. Flexural mode resonators

The second type of device is the flexural mode resonator. It is a triple arm tuning fork where the anti-symmetric out-of-plane deflection is induced by the piezoelectric layer covering each arm (Fig.1b). For resonators smaller than $1000 \times 1000 \text{ } \mu\text{m}^2$, the resonance frequency can be set between 20 to 150kHz.

III. EXPERIMENTAL

A. Fabrication of AlN/Si resonators

Both types of resonators are built from a (100) oriented Silicon on Insulator (SOI) substrate. Figure 2 shows the cross section of the vibrating structure. It consists mainly of single crystal silicon that is oxidized on both sides, and that is topped by AlN and its electrodes.

The piezoelectric sandwich is deposited with the same methods applied in the production of thin film BAW filters [7]. Polycrystalline piezoelectric (002) AlN films are deposited by magnetron sputtering on Pt (111). All thin films are patterned by standard photolithography and dry etching. The Si beams are created by deep reactive ion etching (DRIE) of the Si device layer from the top side, followed by the DRIE of the Si handle from the backside. Figure 3 shows some flexural resonators after processing.

A special dry etching process with a slow etch rate has been used to trim the buried silicon oxide thickness of the flexural resonators.

After the fabrication and dicing, the resonators are wire-bonded and packaged under vacuum in standard metal cans.

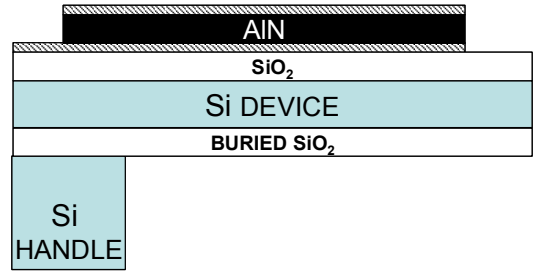


Figure 2. Cross section of Pt/AlN/Pt/SiO₂/Si/SiO₂ device.



Figure 3. Top view of flexural resonators.

B. Characterization of resonators

Because they are piezoelectric, the resonators can be driven and measured with a single set of electrodes. Typically, the AC driving voltage is less than 100 mV. The resonators have been measured using an Agilent 4294A impedance analyzer, which provides a sinusoidal actuation signal to the electrodes, while simultaneously measuring the response of the resonator. The frequency of the actuation signal is swept over a frequency range and the amplitude and phase of the response is recorded. DC bias has been applied in some case in order to observe the variation of resonance frequency. This phenomenon is due to the stiffening of the AlN layer by the DC field.

The coupling coefficient and the Q-factor of the resonator are calculated in the following way. The measured curve is fitted with the equivalent circuit shown in Fig. 4. The fit is performed directly by the impedance analyzer, which delivers the values of the 4 lumped elements. Then the following relations are used to obtain the coupling k_{eff}^2 and series quality factor Q_s :

$$Q_s = \frac{\omega_s L_m}{R_m}$$

with ω_s being the resonance pulsation.

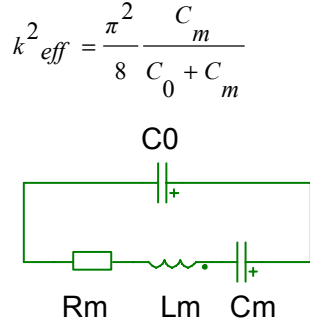


Figure 4. Equivalent circuit of a resonator

The frequency-temperature dependence curve of a resonator can be expressed as:

$$F_1 = F_0 (1 + \alpha \Delta T + \beta \Delta T^2 + \gamma \Delta T^3 + \dots)$$

where :

$\Delta T = T - T_0$

T = temperature

T_0 = reference temperature

F_0 = frequency at T_0

α = first-order temperature coefficient

β = second-order temperature coefficient

γ = third-order temperature coefficient.

TCFs have been obtained by measuring the resonance frequency from -5°C to 55°C . Each temperature step has been stabilized at least for 30 minutes before starting the measurement and an average of at least 5 measurements has been calculated. A polynomial fit is used to extract the temperature coefficients.

IV. RESULTS

A. High Q extensional resonator

Si resonators in extensional mode, oriented along $\langle 110 \rangle$ with a thickness of 100 microns, and activated by 2 micrometers of AlN, exhibit a Q factor under vacuum above 10^5 and k_{eff}^2 around 0.06%. The measured impedance is close to 960 kHz, and the TCf is dominated by the first linear term α , at $-28.25 \text{ ppm}/^\circ\text{C}$. For resonators having the same design but oriented along $\langle 100 \rangle$, which is less stiff, the resonance frequency is around 870 kHz, the TCf value is $27.75 \text{ ppm}/^\circ\text{C}$, and Q is reduced to 50000. For both orientations the Q factor in air is between 6000 and 12000, and increases significantly once the pressure drops below 0.1 mbar.

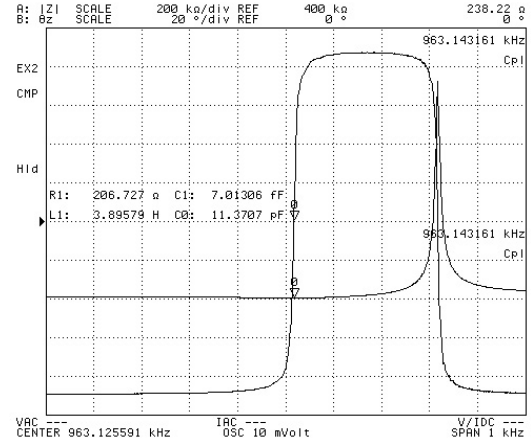


Figure 5. Impedance plot of extensional resonator at $F_{res}=966 \text{ kHz}$ ($Q=120\,000$ under vacuum).

B. Thermally compensated tuning forks

Three arms tuning forks are operating in a flexural out-of-plane mode. A model has been developed to optimize the dimensions of the resonator in order to set the resonance frequency between 20 and 100 kHz. The measured Q factors are not as high as those of the extensional resonators, with values under vacuum in the 3000-5000 range. However, the coupling coefficient is much larger, at 0.2 to 1.1 %. The thermal compensation is achieved at the device level by balancing the positive and negative TCEs of the thin films used in the resonator (AlN, Si, and electrodes with negative TCEs, SiO_2 with a positive TCE).

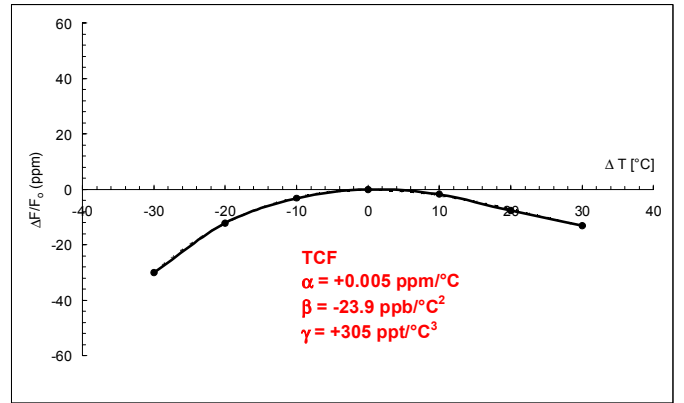


Figure 6. Variation of resonance frequency as a function of temperature for a flexural resonator at 70kHz.

Figure 6 presents the shift of the resonance frequency as a function of temperature ($25^\circ\text{C} \pm 30^\circ\text{C}$) for a triple tuning fork resonating at 70kHz ($Q_{vac} = 4000$, $k_{eff}^2 = 0.21\%$). For this resonator geometry, by adjusting the relative thickness of SiO_2 and AlN/Si multilayer, the first order coefficient of the thermal drift has been brought nearly to zero. This

compensation scheme has been validated with resonators having resonance frequencies ranging from 20 to 100 kHz.

By fabricating these flexural resonators with a total thickness of SiO₂ (top and buried layers) that is slightly larger than necessary, it is possible to fine tune the TCf by removing selectively some of the buried oxide. This trimming procedure has been applied at the die level in this paper, but it could be extended to a wafer level process to enhance production yield. In that case, an ion beam etching system should be used, such as what is currently used for mass production of AlN BAW filters.

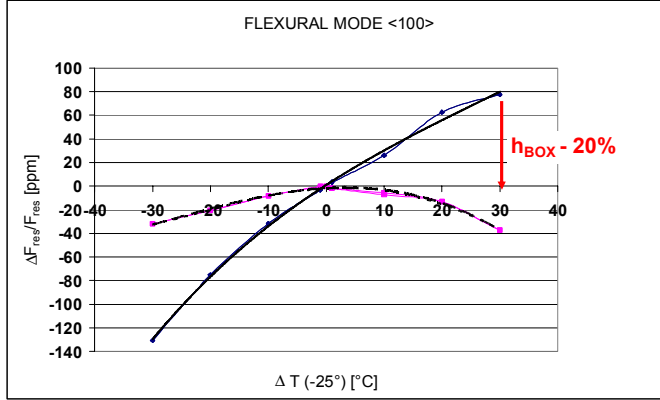


Figure 7. Decreasing of TCf by adjusting the thickness of the buried oxide (flexural resonator at 70kHz).

This trimming concept is shown in Fig. 7, where a quasi null first order TCf could be obtained by adjusting the thickness of buried oxide (slow rate dry etching). The etching of 20% of the initial oxide thickness from the backside results in decreasing α from +3.5 to 0.2 ppm/°C.

Another method for adjusting the resonance frequency of the flexural resonator consists in applying a DC bias during operation. The DC field induced in the piezoelectric layer increases the stiffness of the device and hence increases its resonance frequency.

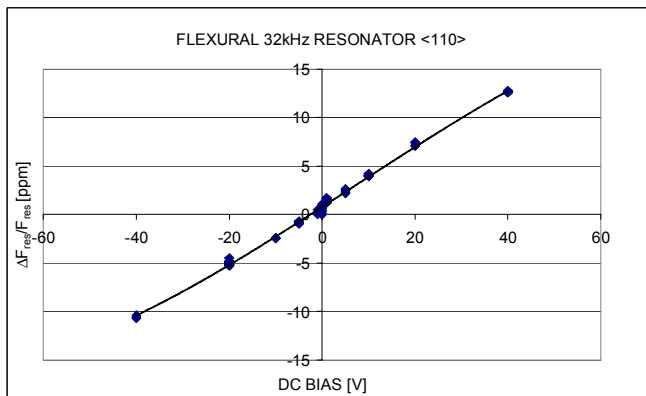


Figure 8. Variation of resonance frequency in function of DC bias (flexural resonator at 70kHz).

An example is shown in Fig. 8 for a flexural resonator operating at 32kHz. Applying a DC bias ranging from -40 to +40V induces a shift of the resonance frequency by +/-12 ppm.

V. CONCLUSIONS

Two types of silicon resonators with AlN piezoelectric activation have been demonstrated in this paper. The first type, the extensional mode resonator, exhibits a Q factor in vacuum as high as 120000 and a mainly linear TCf of -28.5+/-1ppm/°C. The second type, a triple tuning fork, presents a zero first order TCf that has been obtained at the device level by balancing the negative TCEs of Si and AlN with the positive TCE of SiO₂.

Finally, the possibility of fine tuning the TCf by trimming the thickness of SiO₂ has been shown, as well as the ability to adjust the resonance frequency by applying a DC bias, with a sensitivity of 0.3ppm/V.

ACKNOWLEDGMENT

Authors acknowledge F. Martin and D. Ruffieux as well as the staff of the Center of Micro and Nanotechnologies (CMI) at EPFL, Switzerland for technical support.

REFERENCES

- [1] C. T.-C. Nguyen, "Frequency-selective MEMS for miniaturized lowpower communication devices," IEEE Trans. Microwave Theory Tech., vol. 47, pp. 1486-1503, Aug. 1999.
- [2] C. Bourgeois, E. Steinsland, N. Blanc, N. F. de Rooij, "Design of Resonators for The Determination of the Temperature Coefficients of Elastic Constants of Monocrystalline Silicon", Proc. 51st Annual Frequency Control Symposium, 791-799, (1997).
- [3] M. Hopcroft, R. Melamud, R.N. Candler, Woo-Tae Park, B. Kim, G. Yama, A. Partridge, M. Lutz, T.W. Kenny, "Active temperature compensation for micromachined resonators", Solid-State Sensor, Actuator and Microsystems Workshop, Hilton Head Island, South Carolina, June 6-10, 2004, p.364-367.
- [4] W.T.Hsu C.T.-C.Nguyen, "Stiffness-compensated temperature-insensitive micromechanical resonators", The Fifteenth IEEE International Conference on Micro Electro Mechanical Systems, 2002, 731 - 734.
- [5] R. Melamud, B. Kim, M. Hopcroft, S. Chandorkar, M. Agarwal, C.M. Jha, T.W. Kenny, "Composite flexural-mode resonator with controllable turnover temperature", MEMS 2007, Kobe, Japan, 199-202.
- [6] V. Kaajakari, T. Mattila, A. Oja, J. Kiihamäki, H. Seppä "Square-Extensional Mode Single-Crystal Silicon Micromechanical Resonator for Low-Phase-Noise Oscillator Applications", IEEE Electron Device Letters, Vol. 25, No. 4, April 2004, 173
- [7] M.-A. Dubois, J.-F. Carpentier, P. Vincent, C. Billard, G. Parat, C. Muller, P. Ancy, P. Conti, "Monolithic above-IC resonator technology for integrated architectures in mobile and wireless communication" IEEE Journal of Solid State Circuit, 2006, Vol 41, 7-16.